EXHIBIT B

Cell, Vol. 110, 385–397, August 9, 2002, Copyright ©2002 by Cell Press

Directed Differentiation of Embryonic Stem Cells into Motor Neurons

Hynek Wichterle,[1] Ivo Lieberam,[1]
Jeffery A. Porter,[2] and Thomas M. Jessell[1,3]
[1]Howard Hughes Medical Institute
Department of Biochemistry and Molecular Biophysics
Columbia University
New York, New York 10032
[2]Curis, Inc.
61 South Moulton Street
Cambridge, Massachusetts 02138

Summary

Inductive signals and transcription factors involved in motor neuron generation have been identified, raising the question of whether these developmental insights can be used to direct stem cells to a motor neuron fate. We show that developmentally relevant signaling factors can induce mouse embryonic stem (ES) cells to differentiate into spinal progenitor cells, and subsequently into motor neurons, through a pathway recapitulating that used in vivo. ES cell-derived motor neurons can populate the embryonic spinal cord, extend axons, and form synapses with target muscles. Thus, inductive signals involved in normal pathways of neurogenesis can direct ES cells to form specific classes of CNS neurons.

Introduction

Hundreds of distinct neuronal types are generated during the development of the vertebrate central nervous system (CNS), establishing diversity that is essential for the formation of neuronal circuits. The degeneration of specific classes of CNS neurons underlies many neurological disorders, a realization that has prompted interest in defining progenitor cell populations that serve as replenishable sources of neurons for the treatment of neurodegenerative diseases. Directing progenitor cells along specific pathways of neuronal differentiation in a systematic manner has, however, proved difficult, not least because the normal developmental pathways that generate most classes of CNS neurons remain poorly defined.

Studies of the neurogenic potential of progenitor cells have focused on three major classes of cells: neural progenitors derived from embryonic or adult nervous tissue (Alvarez-Buylla et al., 2001; Gage, 2000; Uchida et al., 2000), nonneural progenitor cells derived from other tissues and organs (Brazelton et al., 2000; Mezey et al., 2000; Terada et al., 2002; Ying et al., 2002), and embryonic stem (ES) cells (Bain et al., 1995; Reubinoff et al., 2001; Zhang et al., 2001; Rathjen et al., 2002). ES cells possess the capacity to generate neurons and glial cells, which in some instances express markers characteristic of specific classes of neurons, for example, midbrain dopaminergic neurons (Kawasaki et al., 2000; Lee et al., 2000). Despite these advances, the extent to which the generation of specific neuronal cell types from ES cells recapitulates normal programs of neurogenesis is not clear.

Spinal motor neurons (MNs) represent one CNS neuronal subtype for which pathways of neuronal specification have been defined (Jessell, 2000; Lee and Pfaff, 2001). The generation of MNs appears to involve several developmental steps (Figure 1A). Ectodermal cells acquire an initial rostral neural character through the regulation of BMP, FGF, and Wnt signaling (Munoz-Sanjuan and Brivanlou, 2002; Wilson and Edlund, 2001). These rostral neural progenitors acquire a spinal positional identity in response to caudalizing signals that include retinoic acid (RA) (Durston et al., 1998; Muhr et al., 1999). Subsequently, spinal progenitor cells acquire a MN progenitor identity in response to the ventralizing action of Sonic hedgehog (Shh) (Briscoe and Ericson, 2001).

The specification of MN progenitors by Shh signaling is mediated through the patterned expression of homeodomain (HD) and basic helix-loop-helix (bHLH) transcription factors (Briscoe and Ericson, 2001). At a relatively high level of Shh signaling, a discrete progenitor domain—the pMN domain—is established, and within this domain, cells appear committed to the generation of MNs rather than interneurons (Briscoe et al., 2000). Progenitor cells in the pMN domain are characterized by the expression of two HD proteins, Pax6 and Nkx6.1, and a bHLH protein, Olig2 (Ericson et al., 1997; Sander et al., 2000; Vallstedt et al., 2001; Novitch et al., 2001; Mizuguchi et al., 2001). Each of these transcription factors has an essential role in the specification of spinal MN identity (Ericson et al., 1997; Sander et al., 2000; Vallstedt et al., 2001; Novitch et al., 2001; Mizuguchi et al., 2001; Zhou and Anderson, 2002; Lu et al., 2002). Moreover, their combined activities drive MN progenitors out of the cell cycle (Novitch et al., 2001; Mizuguchi et al., 2001) and direct the expression of downstream transcription factors, notably the HD protein HB9, that consolidate the identity of postmitotic MNs (Pfaff et al., 1996; Arber et al., 1999; Thaler et al., 1999).

These findings have raised the question of whether insights into normal pathways of neurogenesis can be applied in a rational manner to direct heterologous sets of progenitor cells, such as ES cells, into specific CNS neuronal subtypes. ES cells have been reported to generate cells with some of the molecular characteristics of MNs (Renoncourt et al., 1998), but neither the pathway of generation of these neurons nor their developmental potential in vivo have been explored. In this study, we have examined whether the signaling factors that operate along the rostrocaudal and dorsoventral axes of the neural tube to specify MN fate in vivo can be harnessed in vitro to direct the differentiation of mouse ES cells into functional MNs.

[3]Correspondence: tmj1@columbia.edu

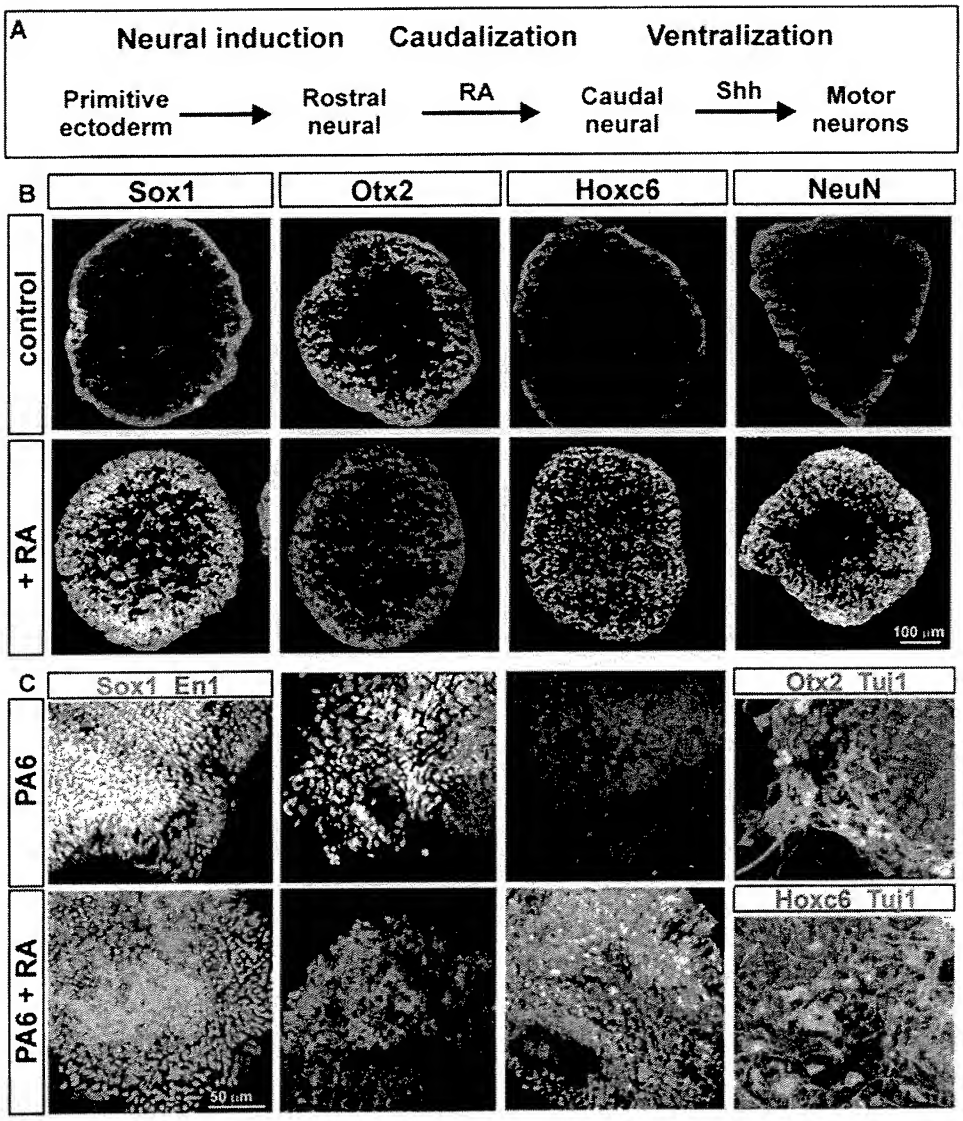

Figure 1. Retinoic Acid Specifies Spinal Progenitor Identity

(A) Progressive steps in MN specification. Neural inductive signals convert primitive ectodermal cells to a rostral neural fate. Signals including retinoic acid (RA) convert rostral neural cells to more caudal identities. Spinal progenitors are converted to MNs by Sonic hedgehog (Shh) signaling. For details see text.

(B) Expression of panneural and rostrocaudal markers in EBs grown in the presence or absence of RA (2 μM). Typically, RA-exposed EBs grown for 3 days contained 40%–60% $Sox1^+$ cells, and EBs grown for 5–7 days contained 50%–70% $NeuN^+$ neurons. Our results do not exclude the presence of some nonneural cells in RA-exposed EBs.

(C) Expression of panneural and rostrocaudal markers in ES cells cultured on PA6 cells for 6 days in the presence or absence of RA (2 μM) (see Supplemental Figure S1).

Results

RA Caudalizes Neural Progenitor Cells in Embryoid Bodies

To begin to examine the capacity of ES cells to generate MNs, we grew mouse ES cells in aggregate culture for 2 days to form embryoid bodies (EBs) (Bain et al., 1995). EBs consisting initially of ~1000 cells were maintained in suspension culture for a further 1 to 7 days in the presence or absence of added factors.

Under control conditions, EBs grown for 2 to 3 days contained few if any cells that expressed the panneural progenitor marker Sox1 (Figure 1B; Pevny et al., 1998; Wood and Episkopou, 1999). Similarly, EBs examined at 5 days contained few if any neurons, assessed by expression of NeuN and a neuronal β-tubulin isoform recognized by MAb TuJ1 (Figure 1B, data not shown). In contrast, exposure of EBs to RA (100 nM to 2 μM) for 2 to 3 days resulted in the presence of many $Sox1^+$ cells (Figure 1B), and by 5 days, many $NeuN^+$, $TuJ1^+$ postmitotic neurons were detected (Figure 1B, data not shown).

We determined the rostrocaudal positional identity of the neural progenitor cells formed in RA-exposed EBs

by assaying expression of Otx2 and En1, the coexpression of which is indicative of early midbrain identity (Davis and Joyner, 1988; Mallamaci et al., 1996), and the expression of Hoxc5, Hoxc6, and Hoxc8, markers of spinal cord identity (Belting et al., 1998; Liu et al., 2001). Cells in EBs exposed to RA for 3 days lacked Otx2 and En1 expression and expressed Hoxc5 and Hoxc6, but not Hoxc8 (Figure 1B, data not shown). This profile of neural Hox-c expression is indicative of spinal cord cells with a rostral cervical character (Belting et al., 1998; Liu et al., 2001).

Since exposure of ES cells to RA promotes neural differentiation and the expression of spinal positional markers, this protocol did not permit a direct test of the caudalizing action of RA on ES-derived neural cells. We therefore neuralized ES cells through a RA-independent pathway, using the PA6 stromal cell line as source of neural inductive signals (Kawasaki et al., 2000). Mouse ES cells grown on a monolayer of PA6 cells for 5 days generated numerous Sox1$^+$ cells, many of which expressed Otx2 and En1, but no cells expressed Hoxc5 or Hoxc6 (Figure 1C, data not shown). By 6 days, many Otx2$^+$, TuJ1$^+$ neurons were detected (Figure 1C). Addition of RA (2 μM) to ES cells grown on PA6 cells still resulted in the generation of many Sox1$^+$ cells, but these cells lacked Otx2 and En1 expression, and many now expressed Hoxc5 and Hoxc6 (Figure 1C, data not shown). These findings indicate that, as in vivo (Muhr et al., 1999), neuralized ES cells of an initial midbrain-like character can be caudalized to a spinal character upon exposure to RA.

Hh Dependence of Motor Neuron Progenitor Specification in Caudalized Embryoid Bodies

To examine whether the spinal progenitors present in RA-exposed EBs can differentiate into MN progenitors, we monitored the expression of HD and bHLH transcription factors that delineate sets of neural progenitor cells positioned along the dorso-ventral axis of the neural tube (Figures 2A and 2B; Briscoe and Ericson, 2001). Spinal MN progenitors are found within the pMN domain and express Pax6, Nkx6.1, and Olig2 and exclude Pax7, Irx3, Dbx1, and Nkx2.2 (Figure 2B, data not shown). Many cells in EBs exposed to RA for 3 days expressed Pax7, Pax6, Irx3, and Dbx1, and few cells expressed Nkx6.1, Olig2, or Nkx2.2 (Figures 2C and 2D, data not shown). This profile of transcription factor expression is characteristic of progenitor cells located in the dorsal and intermediate spinal cord that give rise to interneurons (Figure 2B; Lee and Jessell, 1999).

The induction of MN progenitors depends on Shh activity (Briscoe and Ericson, 2001). We therefore examined whether Shh signaling changes the profile of progenitor cell transcription factor expression in RA-exposed EBs. To activate the Shh signaling pathway, we used a specific small molecule agonist of Shh signaling, Hh-Ag1.3 (M. Frank-Kamenetsky and J.A.P., unpublished data), or recombinant Shh-N protein (Roelink et al., 1995), with essentially identical results. Joint exposure of EBs to RA and 10 nM Hh-Ag1.3 for 3 days repressed Pax7 expression, increased the number of Pax6$^+$ and Irx3$^+$ cells, reduced the number of Dbx1$^+$ cells, and induced a few Nkx6.1$^+$ and Olig2$^+$ cells (Figures 2C and 2D, data not shown). Joint exposure of EBs to RA and 1 μM Hh-Ag1.3 virtually eliminated Dbx1 expression, markedly reduced the number of Irx3$^+$ and Pax6$^+$ cells, and induced many Nkx6.1$^+$ and Olig2$^+$ cells (Figures 2C and 2D). Olig2$^+$ cells in Hh-Ag1.3-exposed EBs incorporated BrdU (see Supplemental Figure S2 at http://www.cell.com/cgi/content/full/110/3/385/DC1), indicating that they are cycling progenitors. At this concentration of Hh-Ag1.3, a few Nkx2.2$^+$ cells were induced (Figures 2C and 2D), but no HNF3β$^+$ floor plate cells were detected (data not shown). The dorsal-to-ventral shift in the profile of expression of progenitor cell transcription factor markers in EBs in response to Hh signaling closely resembled the behavior of neural tube progenitors (Ericson et al., 1996, 1997; Briscoe et al., 2000). In particular, high levels of Shh signaling generated many cells that expressed a profile of HD and bHLH proteins characteristic of MN progenitors.

To determine whether MNs are generated from the caudalized and ventralized progenitor cells present in RA- and Hh-exposed EBs, we analyzed the expression of HB9, a HD protein expressed selectively and persistently by somatic MNs (Figure 3A; Pfaff et al., 1996; Arber et al., 1999; Thaler et al., 1999). RA-exposed EBs grown alone for 5 days did contain a few HB9$^+$ neurons (Figure 3B; 7 ± 2 HB9$^+$ neurons/section). To test whether these neurons are generated in a Hh-dependent manner, we grew RA-exposed EBs in the presence of a function blocking anti-Hh antibody (MAb 5E1 Ig 30 μg/ml; Ericson et al., 1996). No HB9$^+$ neurons (Figure 3B) were detected under these conditions, indicating that an endogenous source of Hh is required for the differentiation of the few MNs found in RA-exposed EBs.

Conversely, we examined whether the efficiency of MN generation can be enhanced by elevating the level of Hh signaling in RA-exposed EBs. Exposure of RA-treated EBs to Shh (300 nM) or Hh-Ag1.3 (1 μM) resulted in a marked increase in the number of MNs generated: typically 20%–30% of cells in these EBs expressed HB9 (~5000 HB9$^+$ neurons; 509 ± 57 HB9$^+$ neurons/section; ~10–15 sections per EB) (Figure 3B, data not shown). These HB9$^+$ cells coexpressed NeuN and TuJ1 (Figures 3C and 3D) and did not incorporate BrdU (see Supplemental Figure S2 at http://www.cell.com/cgi/content/full/110/3/385/DC1), indicating that they are postmitotic neurons. No HB9$^+$ neurons were generated in EBs treated with Hh-Ag1.3 (1 μM) for 5 days without RA exposure (Figure 3B). Thus, the generation of MNs in EBs depends on both the caudalizing action of RA and the ventralizing action of Hh.

To define the molecular character of postmitotic MNs, we examined the expression of three LIM HD proteins expressed by subsets of spinal motor neurons—Isl1, Lhx3, and Lim1 (Figure 3A; Tsuchida et al., 1994; Sharma et al., 1998; Kania et al., 2000). All three proteins were expressed by HB9$^+$ MNs in RA- and Hh-exposed EBs. Over 70% of HB9$^+$ motor neurons coexpressed Isl1 and Lhx3 (Figures 3E and 3F), but a much smaller fraction (<5%) coexpressed Lim1 (Figure 3G). No Isl1$^+$ neurons coexpressed Phox2b (data not shown), a marker of hindbrain visceral MNs (Pattyn et al., 2000). The low proportion of MNs that coexpressed HB9 and Lim1—a profile indicative of lateral motor column (LMC) neurons (Kania et al., 2000)—is consistent with the rostral cervical iden-

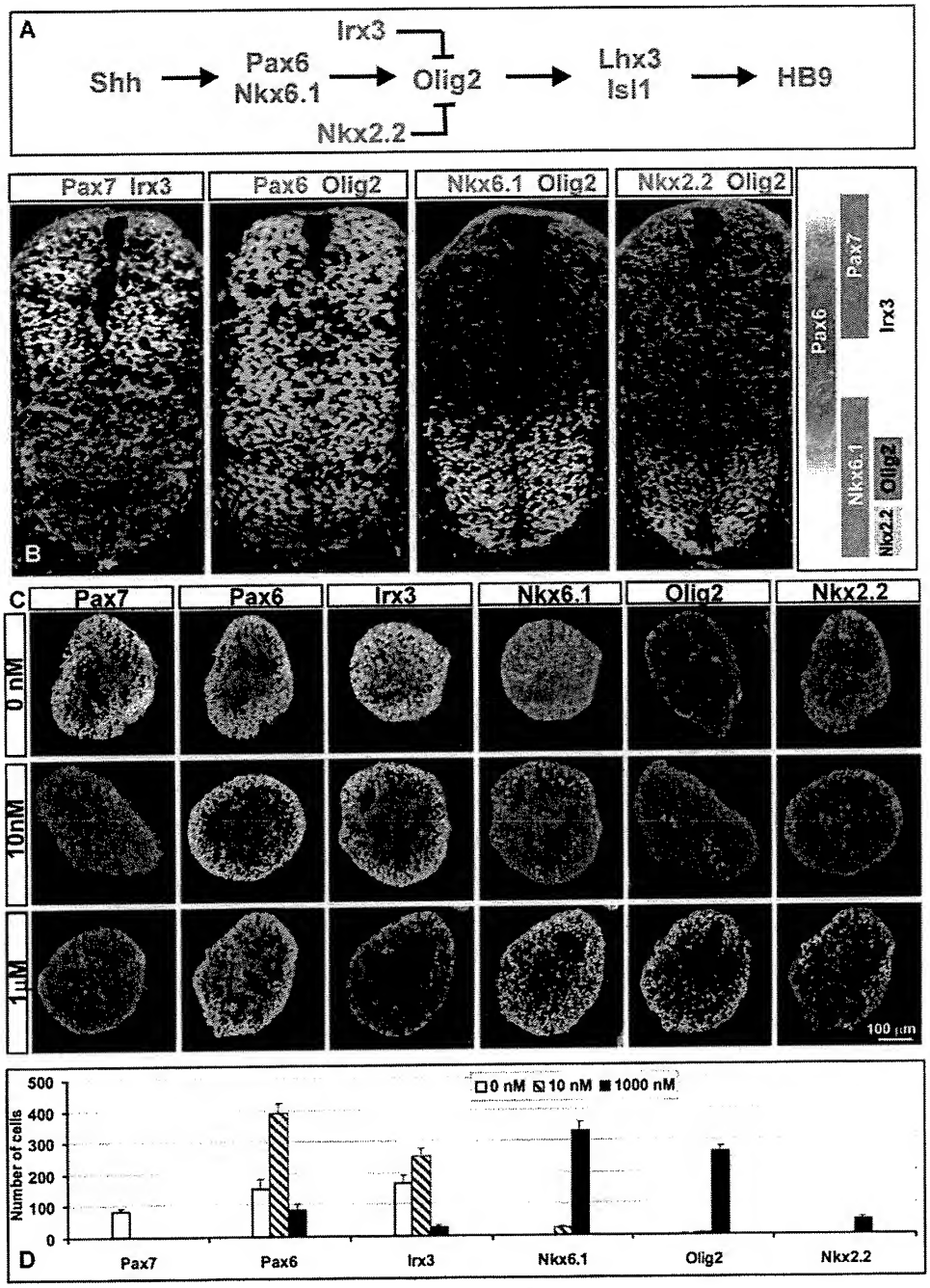

Figure 2. Hedgehog-Dependent Ventralization of Neural Progenitor Cells in Embryoid Bodies

(A) Shh-activated transcriptional pathway of spinal MN generation. Proteins that promote and inhibit MN generation are shown in red and blue, respectively.

(B) Expression of HD and bHLH proteins in the caudal neural tube of E9.5 mouse embryos. Progenitors in the domain giving rise to MNs express Olig2, Nkx6.1, and low levels of Pax6.

(C) Transcription factor expression in ES cell-derived EBs grown for 3 days in the presence of RA (2 μM) alone, and with 10 nM or 1 μM Hh-Ag1.3.

(D) Quantitation of transcription factor expression in EBs in the presence of RA and Hh-Ag1.3. Mean ± SEM, number of cells per section from eight EBs assayed.

tity revealed by the profile of Hox-c protein expression (Belting et al., 1998; Liu et al., 2001).

Since Shh acts in a graded manner, ventral interneurons are induced at concentrations only slightly below that sufficient for MN generation (Briscoe and Ericson, 2001). We therefore examined whether ventral interneurons are also generated in RA-treated EBs exposed to 1 μM Hh-Ag1.3. Both Lhx3$^+$, Chx10$^+$ V2 neurons and Lim1/2$^+$ (likely V0 and V1) neurons were detected in these EBs (Figures 3G and 3H, data not shown). Thus, as

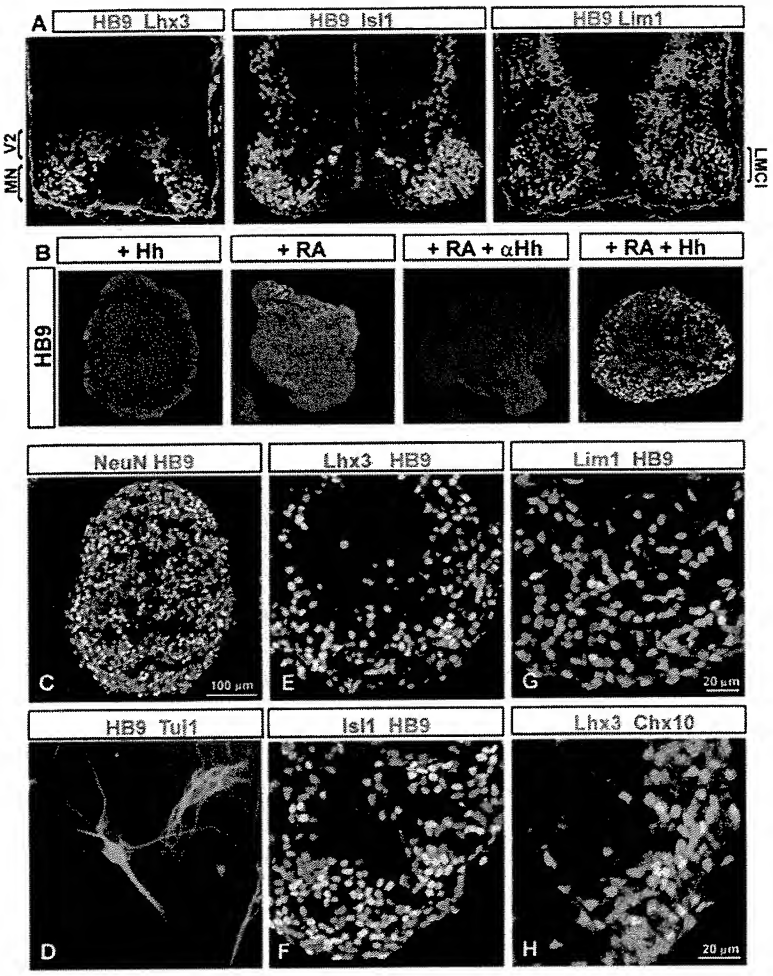

Figure 3. Expression of Motor Neuron and Interneuron Transcription Factors in Embryoid Bodies

(A) Coexpression of HB9 and Lhx3 in a subset of MNs. Lhx3 is also expressed by V2 interneurons. Neurons in the lateral division of the LMC express high levels of HB9 in the absence of Isl1, whereas medial LMC neurons express Isl1 and low levels of HB9. Coexpression of HB9 and Lim1 defines lateral LMC neurons. Many interneurons express Lim1 and Lim2, and some express Isl1.

(B) EBs grown for 5 days with Hh-Ag1.3 (1 μM) but not RA do not contain HB9$^+$ neurons. EBs grown for 5 days with RA (2 μM) and without Hh-Ag1.3 contain a few HB9$^+$ neurons. EBs grown for 5 days with RA and anti-Hh (MAb 5E1; 30 μg/ml) do not contain HB9$^+$ neurons. EBs grown for 5 days with RA and Shh-N (300 nM) (Hh) contain many HB9$^+$ neurons.

(C) Coexpression of HB9 and NeuN in neurons in EBs grown for 5 days with RA and Hh-Ag1.3 (1 μM).

(D) Localization of HB9 in a TuJ1$^+$ neuron, obtained by dissociation of EBs grown for 5 days with RA, and cultured for a further 2 days.

(E) Coexpression of HB9 and Lhx3 in neurons in EBs grown for 5 days with RA and Hh-Ag1.3 (1 μM). Cells that express Lhx3 alone are V2 interneurons.

(F) Coexpression of HB9 and Isl1 in MNs in EBs grown for 5 days with RA and Hh-Ag1.3 (1 μM).

(G) HB9 and Lim1 are coexpressed in few neurons in EBs grown for 5 days with RA and Hh-Ag1.3 (1 μM). Cells that express Lim1 alone are interneurons.

(H) Coexpression of Chx10 and Lhx3 in V2 interneurons in EBs grown for 5 days with RA and Hh-Ag1.3 (1 μM).

with primary neural tissue (Briscoe and Ericson, 2001), small variations in the level of Hh signaling to which cells in EBs are exposed results in the generation of both ventral interneurons and spinal MNs.

Generation and Isolation of eGFP-Labeled, ES Cell-Derived Motor Neurons

The heterogeneity of ventral neurons induced in EBs by RA and Hh signaling prompted us to develop a method for identifying, purifying, and manipulating ES cell-derived MNs. We designed an ES cell line capable of giving rise to MNs identifiable by expression of enhanced green fluorescent protein (eGFP). A transgenic mouse line was generated in which an *eGfp* cDNA was expressed under the control of the mouse *HB9* promoter (Figure 4A; Arber et al., 1999). Transgenic founder mice were screened by comparison of the patterns of HB9 and eGFP expression. One mouse line, *mHB9-Gfp1b*, expressed high levels of eGFP in the cell bodies of spinal MNs in E9.5–P10 mice, in a pattern that paralleled that of endogenous HB9 (Figures 4B–4G). In addition, eGFP expression was detected at high levels in the axons and dendrites of MNs (Figure 4C, data not shown). An ES cell line (HBG3) was derived from *mHB9-Gfp1b* transgenic mice, and these cells transmitted the *eGfp* gene through the germline and directed expression of eGFP in a similarly MN-selective pattern (data not shown).

EBs generated from HBG3 ES cells grown for 5 days in RA, but without Hh-Ag1.3, contained a few HB9$^+$ MNs, and all of these coexpressed eGFP in their cell somata and neurites (Figure 5A). The number of eGFP$^+$/HB9$^+$ MNs was increased upon exposure to Hh-Ag1.3 in a concentration-dependent manner (Figures 5B and 5C). Typically, eGFP$^+$/HB9$^+$ MNs constituted 20%–30% of the total number of cells present in EBs exposed to RA and 1 μM Hh-Ag1.3 (Figure 5C). Exposure of EBs to Hh-Ag1.3 (1 μM) in the absence of RA failed to generate eGFP$^+$/HB9$^+$ MNs (Figure 5C). Thus, HBG3 ES cells can also be induced to generate eGFP$^+$/HB9$^+$ MNs in an efficient manner, through activation of RA and Hh signaling pathways.

We used eGFP expression to test whether HBG3 ES cell-derived MNs undergo aspects of differentiation in vitro that are characteristic of embryo-derived MNs. RA- and Hh-exposed EBs (Figure 5D) were dissociated into single cells or into small aggregates and plated on a matrigel substrate in the presence of neurotrophic factors. ES cell-derived MNs adhered and extended processes that could be identified by eGFP expression (Figures 5E and 5F). The morphological features of these

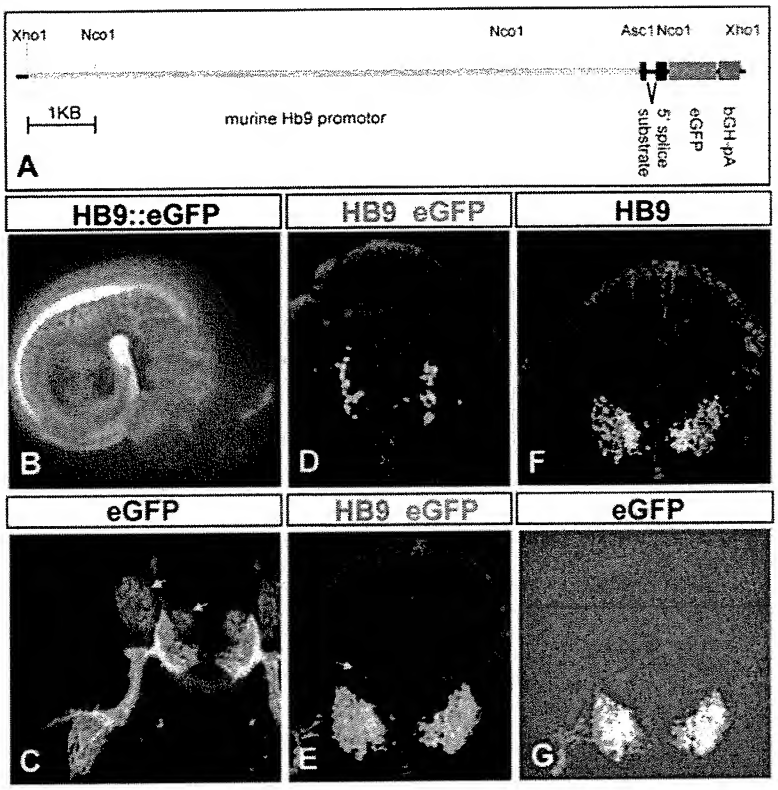

Figure 4. eGFP-Labeled Motor Neurons in Transgenic Mouse Embryos

(A) Construct for generation of *mHB9-Gfp1b* transgenic line.

(B) eGFP expression in an E10.5 *mHB9-Gfp1b* embryo.

(C) eGFP expression in MN cell bodies, dendrites, and axons in E10.5 *mHB9-Gfp1b* embryos. In this line a very low level of expression (10- to 20-fold lower than in MNs) was detected in DRG neurons and a subset of ventral interneurons at e10.5, but not later (arrows in C and E).

(D) HB9 and eGFP expression in cervical spinal cord of E9.5 *mHB9-Gfp1b* embryos.

(E–G) HB9 and eGFP expression in thoracic spinal cord of E10.5 *mHB9-Gfp1b* embryos.

ES cell-derived MNs resembled those of eGFP-labeled MNs isolated from the embryonic spinal cord of *mHB9-Gfp1b* mice (Figures 6J and 6K, data not shown). Moreover, eGFP$^+$/HB9$^+$ MNs generated in vitro expressed choline acetyltransferase (Figures 5G and 5H), indicative of their cholinergic transmitter status.

We also examined the neurotrophic factor dependence of HBG3 ES cell-derived MNs, in a direct comparison with primary embryonic MNs. We dissociated RA- and Hh-exposed HBG3-derived EBs and isolated cells that expressed high levels of eGFP by fluorescence-activated cell sorting (FACS) (Figure 6A). In parallel, we FACS-isolated primary embryonic MNs from rostral cervical spinal cord of E10.5 *mHB9-Gfp1b* embryos (data not shown). From either source, >98% of neurons that expressed high levels of eGFP coexpressed HB9 (Figures 6B and 6C), and these neurons extended long processes (Figures 6D and 6E, data not shown). The survival of purified eGFP$^+$/HB9$^+$ MNs generated from HBG3 ES cells (Figures 6F–6I and 6L) or isolated from E10.5 *mHB9-Gfp1b* embryos (Figures 6J–6L) exhibited a similar dependence on neurotrophic factors (see Bloch-Gallego et al., 1991).

Differentiation of ES Cell-Derived eGFP$^+$ Motor Neurons in Embryonic Spinal Cord

The survival and differentiation of HBG3 ES cell-derived MNs in vitro prompted us to examine the behavior of these neurons when reintroduced into the spinal cord in vivo. EBs were isolated after 3 to 4 days of RA- and Hh-Ag1.3 exposure (when postmitotic MNs first appear), dispersed into small aggregates, and implanted into the prospective rostral or caudal cervical, thoracic, or lumbar levels of the spinal cord of stage 15–17 chick embryos (Figure 7A), a time when the differentiation of endogenous MNs begins (Hollyday and Hamburger, 1977). Operated embryos were permitted to develop for a further 3 to 7 days, to stages 27–36.

Analysis of the spinal cord of operated embryos at stage 27 revealed the presence of many eGFP$^+$/HB9$^+$ MNs (Figures 7B–7J and 7O–7Q). Although the initial dorsoventral placement of EB grafts was not controlled, we detected a striking segregation in the position of mouse MNs and interneurons in the chick spinal cord, when examined 3 to 7 days later (Figure 7E). Almost invariably, eGFP$^+$/HB9$^+$ MNs were found in a ventrolateral position characteristic of that of endogenous MNs, whereas EB-derived Lim2$^+$ interneurons (recognized by a rodent-specific antibody) were scattered along the dorsoventral axis of the spinal cord (Figure 7E). The vast majority of eGFP$^+$/HB9$^+$ MNs coexpressed Lhx3 and lacked expression of Lim1, regardless of the segmental level of grafting (Figure 7F, data not shown). Thus, the LIM HD profile of eGFP$^+$/HB9$^+$ ES cell-derived MNs observed in vitro is not changed by in vivo grafting.

The presence of Olig2$^+$ MN progenitors in grafted EBs raised the possibility that some or all of the eGFP$^+$ ES cell-derived MNs detected in chick spinal cord derived from grafted progenitor cells that underwent terminal differentiation in situ. To test this, we pulse-labeled RA and Hh-Ag1.3-exposed EBs with BrdU immediately prior to grafting. Two days after transplantation, we detected a small proportion of BrdU-labeled eGFP$^+$/HB9$^+$ motor neurons in the chick spinal cord (data not shown), providing evidence that some ventral spinal progenitors in EBs are able to differentiate into motor neurons in vivo.

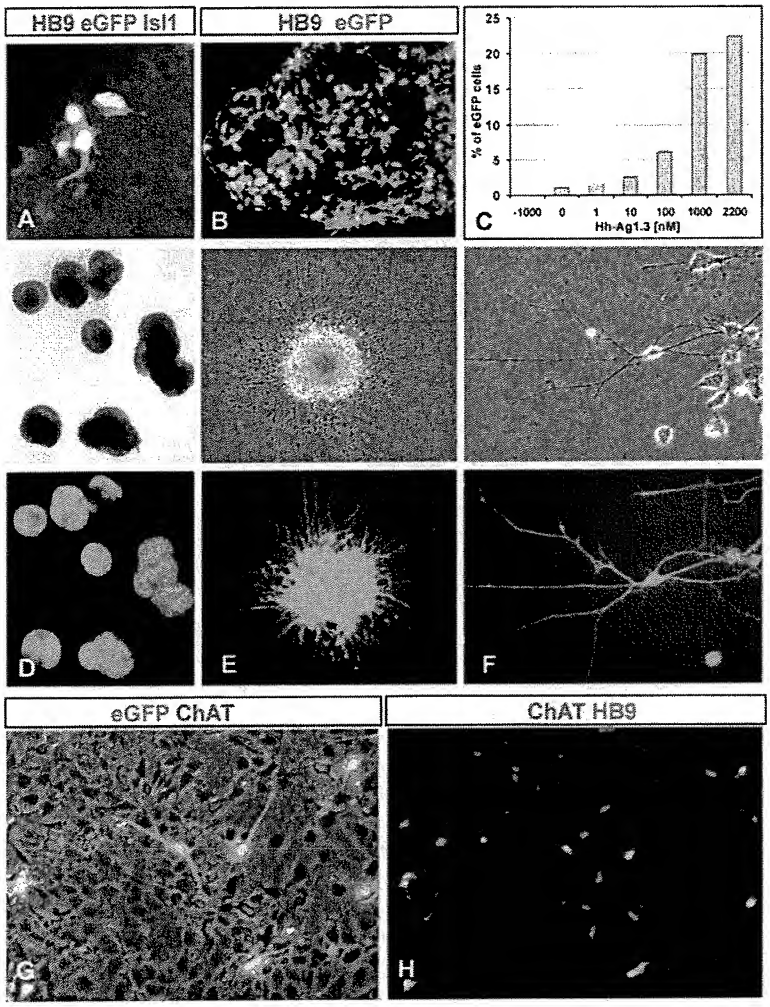

Figure 5. eGFP-Labeled Motor Neurons Derived in Vitro from HBG3 ES Cells

(A) eGFP$^+$ MN cell bodies and axons in EBs grown for 5 days with RA coexpress HB9 and Isl1.

(B) The number of eGFP$^+$, HB9$^+$ MNs is increased upon exposure to RA and Hh-Ag1.3 (1 μM).

(C) Quantitation of eGFP$^+$ MNs in EBs grown for 5 days with RA and Hh-Ag1.3 (0 to 2.2 μM). The point marked as −1000 refers to EBs grown with 1 μM Hh-Ag1.3, but without RA.

(D) Bright-field and fluorescence images showing eGFP expression in EBs grown for 5 days with RA and Hh-Ag1.3 (1 μM).

(E) Phase and fluorescence images showing eGFP$^+$ cells and axons in EBs grown for 5 days with RA and Hh-Ag1.3 (1 μM) and plated on matrigel for 2 days.

(F) Phase and fluorescence images showing eGFP expression.

(G and H) Expression of HB9, eGFP, and choline acetyltransferase (ChAT) in ES cell-derived MNs grown in vitro for 7 days. ChAT$^+$ neurons that lack HB9 and eGFP expression are likely to be interneurons.

In view of this finding, we tested whether postmitotic MNs that had been generated from HBG3 cells in vitro could also survive in the spinal cord in vivo. eGFP$^+$/HB9$^+$ ES cell-derived MNs were isolated from dissociated EBs by FACS sorting and then grafted. After 3 days, many eGFP$^+$/HB9$^+$ MNs were found in the ventral regions of the spinal cord (Figures 7C and 7D). Thus, postmitotic ES cell-derived MNs can also survive and differentiate in vivo.

Certain cell populations have been reported to undergo fusion with somatic cells (Terada et al., 2002; Ying et al., 2002) prompting us to test the possibility that HBG3 ES cell-derived eGFP$^+$/HB9$^+$ MNs might have formed somatic hybrids with chick neurons. We found that eGFP$^+$/HB9$^+$ MN cell bodies expressed neuronal surface proteins of mouse origin, such as NCAM (Figure 7G; recognized by a rodent-specific antibody), but not surface proteins of chick origin, such as SC1 (Figure 7I, recognized by a chick-specific antibody). Similarly, the axons of grafted MNs expressed mouse but not chick surface proteins (Figures 7H and 7J). These findings provide evidence against somatic cell fusion. As an additional control, we examined the fate of grafts of HBG3 EBs that had been neuralized and caudalized by in vitro exposure to RA but prevented from ventralization by inclusion of anti-Hh antibody (5E1, 30 μg/ml). Many mouse NCAM$^+$ cells and Lim2$^+$ interneurons were found, but no eGFP$^+$/HB9$^+$ MNs were detected (Figures 7K–7N). Thus, cells present in RA-exposed EBs are not directed to a MN fate in vivo upon exposure to signals provided by host chick tissues.

We also examined whether the axons of HBG3 ES cell-derived MNs extend along normal motor neuron trajectories. Many eGFP$^+$ axons were detected in the ventral roots (Figures 7B, 7D, and 7O). Analysis of the pattern of peripheral projections of eGFP$^+$ motor axons in stage 27 embryos revealed that HBG3 ES cell-derived MNs grafted at rostral cervical levels projected to axial musculature (data not shown), MNs grafted at thoracic levels projected toward both axial and body wall musculature (Figures 7O and 7P), and MNs grafted at limb levels (caudal cervical or lumbar spinal cord) projected axons into both the dorsal and ventral halves of the limb (Figure 7Q, data not shown). Thus, ES cell-derived MNs are able to populate different segmental levels of the spinal cord and to project along the major peripheral axonal pathways selected by host somatic MNs in vivo.

We also found that the axons of eGFP$^+$ MNs reach muscle targets. For example, extensive ingrowth and branching of eGFP$^+$ motor axons was detected in the

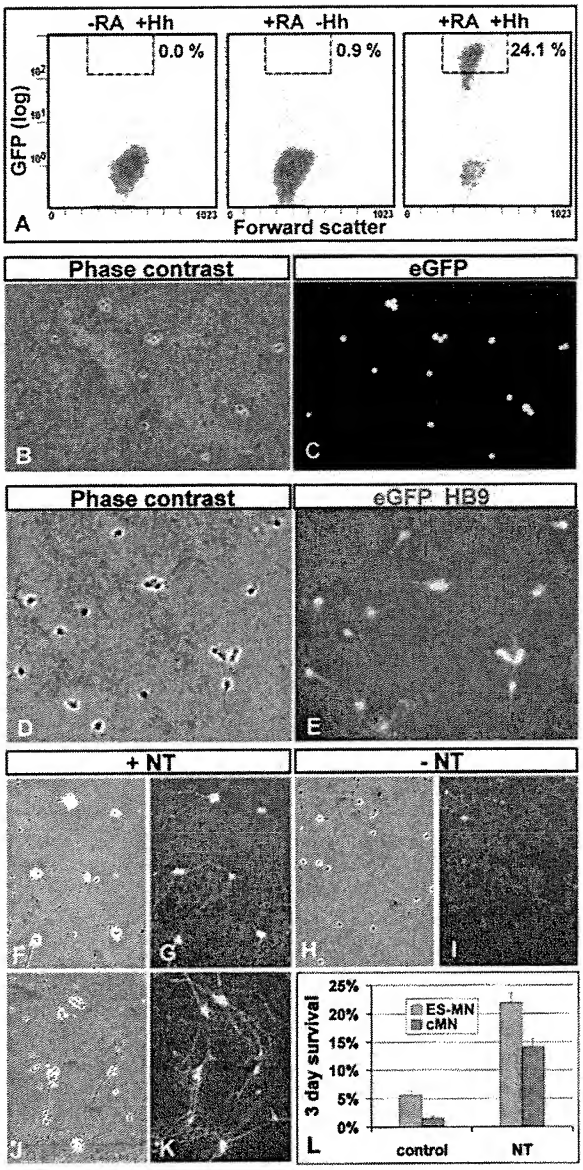

Figure 6. Isolation of eGFP$^+$ ES-Cell Derived Motor Neurons

(A) FACS analysis (density plots) of HBG3 ES cells differentiated with Hh-Ag1.3 (1 μM) alone, with RA (2 μM) alone, or with both factors. Rectangle indicates gate used for sorting eGFP$^+$ MNs.

(B and C) ES cell-derived MNs isolated by FACS express high levels of eGFP.

(D and E) eGFP$^+$ MNs coexpress HB9 and extend neurites on a matrigel substrate, at 24 hr.

(F and G) FACS-sorted ES cell-derived MNs cultured with neurotrophic factors (NT3, BDNF, CNTF, and GDNF) survive for 3 days and extend neurites (F). Surviving MNs maintain expression of eGFP (G).

(H and I) Most FACS-sorted ES cell-derived MNs cultured without neurotrophic factors die within 3 days.

(J and K) FACS-sorted eGFP$^+$ primary MNs from rostral cervical levels also survive and extend eGFP$^+$ axons in the presence of neurotrophic factors.

(L) Primary cervical eGFP$^+$ MNs (cMN) and ES cell-derived eGFP$^+$ MNs (ES-MN) survival (percentage of plated cells) after 3 days in culture in the presence (NT) or absence (control) of neurotrophic factors (mean ± SEM; 6 wells scored).

intercostal muscles at stages 30–35 (Figure 8A). We examined whether these eGFP$^+$ motor axons exhibit aspects of terminal synaptic differentiation at sites of muscle contact. We analyzed three markers of nerve terminal differentiation: synaptobrevin (Syb, recognized by a rodent-specific antibody), the vesicular ACh transporter (VAChT, recognized by a rodent-specific antibody), and synaptotagmin (Syn, recognized by an antibody that detects both rodent and chick proteins). At sites of contact with muscles, eGFP$^+$ motor axon branches displayed signs of presynaptic specialization, as revealed by focal expression of Syb, Syn, and VAChT (Figures 8B–8E).

We next examined whether the presynaptic terminal specializations of eGFP$^+$ motor axons are aligned with postsynaptic specialization of the muscle surface membrane by analyzing the distribution of ACh receptors. Many of the terminal specializations of eGFP$^+$ motor axons were aligned with focal clusters of ACh receptors on the muscle surface, defined by rhodamine-α-bungarotoxin labeling (Figure 8F). Thus, the axons of ES cell-derived MNs appear to form synapses with target skeletal muscles in vivo.

Discussion

We have examined whether the delineation of extracellular inductive signals and transcription factors involved in the conversion of neural progenitor cells to specific neuronal subtypes in vivo permits a rational, embryology-based approach to the differentiation of ES cells into specific classes of CNS neurons. Our findings show that mouse ES cells can generate spinal MNs at high efficiency and that the pathway of MN generation from ES cells recapitulates the steps of MN generation in vivo. ES cell-derived MNs repopulate the ventral spinal cord in vivo, extend axons into the periphery, and form synapses with muscle targets. These studies establish the feasibility of applying insights into normal developmental signaling cascades, in particular the control of extracellular inductive signals, to direct the differentiation of ES cells into specific classes of CNS neurons. The ability of ES cell-derived MNs to innervate target muscle cells offers the potential for a systematic evaluation of the use of such neurons to restore motor function in mammalian models of spinal cord injury and MN degenerative diseases.

The Pathway of Motor Neuron Generation from ES Cells

The specification of MN fate in vivo can be considered in three sequential steps: (1) the primary neuralization of ectodermal cells, (2) the secondary caudalization of neural cells, and (3) the ventralization of caudalized neural cells (Jessell, 2000; Wilson and Edlund, 2001). Our results, discussed below, provide evidence that the pathway of ES cell differentiation into MNs resembles the normal programs involved in the caudalization and ventralization of neural cells.

Neural plate cells, regardless of their final positional identity, appear initially to possess a rostral character (Munoz-Sanjuan and Brivanlou, 2002). The subsequent imposition of a spinal cord character appears to involve

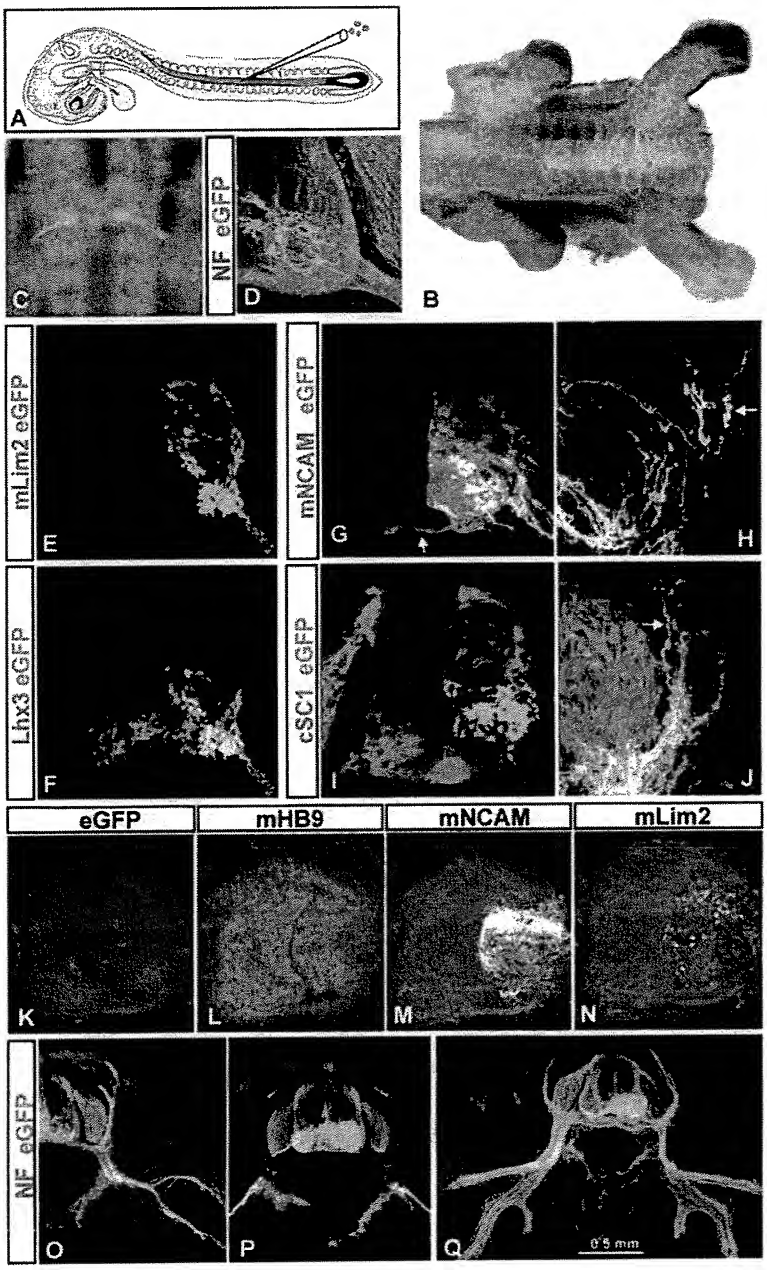

Figure 7. Integration of Transplanted ES Cell-Derived Motor Neurons into the Spinal Cord In Vivo

(A) Implantation of HBG3 ES cell-derived MN-enriched EBs into stage 15–17 chick spinal cord.

(B) Bright-field/fluorescence image showing eGFP$^+$ MNs in thoracic and lumbar spinal cord, assayed at stage 27 (ventral view).

(C and D) Location of FACS-sorted ES-cell derived eGFP$^+$ MNs in thoracic spinal cord, assayed at stage 27. eGFP$^+$ MNs are clustered in the ventral spinal cord (D).

(E–J) Transverse sections through stage 27 chick spinal cord at rostral cervical levels after transplantation of MN-enriched EBs. MNs are concentrated in the ventral spinal cord and are segregated from transplanted interneurons, labeled by a mouse-specific Lim2 antibody (E). Many ES cell-derived MNs coexpress eGFP and Lhx3 (F). ES cell-derived MNs (G) and axons (arrow, H) are labeled by rodent-specific anti-NCAM antibody, but do not express the chick MN marker protein SC1 (I and J). eGFP$^-$, NCAM$^+$ axons cross the floor plate but do not project out of the spinal cord (arrows, G and H).

(K–N) Transverse sections of thoracic spinal cord at stage 27, after grafting EBs grown with RA (2 μM) and anti-Hh antibody (5E1, 30 μg/ml). No mouse-derived MNs were detected either by eGFP (K) or by a mouse-specific anti-HB9 antibody (L). In contrast, many mouse-derived NCAM$^+$ (M) and Lim2$^+$ (N) interneurons are present.

(O–Q) Transverse sections through stage 27 spinal cord at thoracic (O and P) and lumbar (Q) levels after grafting MN-enriched EBs. eGFP$^+$ MNs are concentrated in the ventral spinal cord. Ectopic eGFP$^+$ MNs are located within the lumen of the spinal cord. eGFP$^+$ axons exit the spinal cord primarily via the ventral root and project along nerve branches that supply axial (O–Q), body wall (O and P), and dorsal and ventral limb (Q) muscles. The pathway of axons is detected by neurofilament (NF) expression. eGFP$^+$ axons are not detected in motor nerves that project to sympathetic neuronal targets.

RA-mediated signals provided by the paraxial mesoderm (Muhr et al., 1999; Wilson and Edlund, 2001). In particular, RA has been shown to specify spinal cord character at the expense of midbrain or rostral hindbrain identity (Muhr et al., 1999). We find that ES cells that have been neuralized by exposure to PA6 activity express a midbrain character (see also Kawasaki et al., 2000) but can be converted to a cervical spinal identity upon exposure to RA. This conversion is complemented by a RA-mediated inhibition of midbrain dopaminergic neuronal differentiation (Kawasaki et al., 2000). Together, these findings support the view that RA promotes spinal fate in neuralized EBs in a manner that parallels its normal role in patterning the rostrocaudal axis of the neural tube.

Why do the spinal cord cells induced in EBs by RA possess a rostral cervical positional identity? A likely reason for this comes from the finding that, at times after the specification of a generic spinal progenitor identity, the rostrocaudal identity of spinal cord cells continues to be influenced by ongoing RA signaling (Liu et al., 2001). In particular, RA-mediated signaling promotes the acquisition of rostral cervical spinal positional character, at the expense of thoracic and lumbar positional identities (Liu et al., 2001). Thus, the exposure of neuralized ES cells to RA is likely to account both for the emergence of an initial spinal positional character and for the restriction of these cells to a rostral cervical identity.

ES cells that have acquired a spinal progenitor identity also appear to follow a normal pathway of MN progenitor specification. One line of evidence for this is the sensitiv-

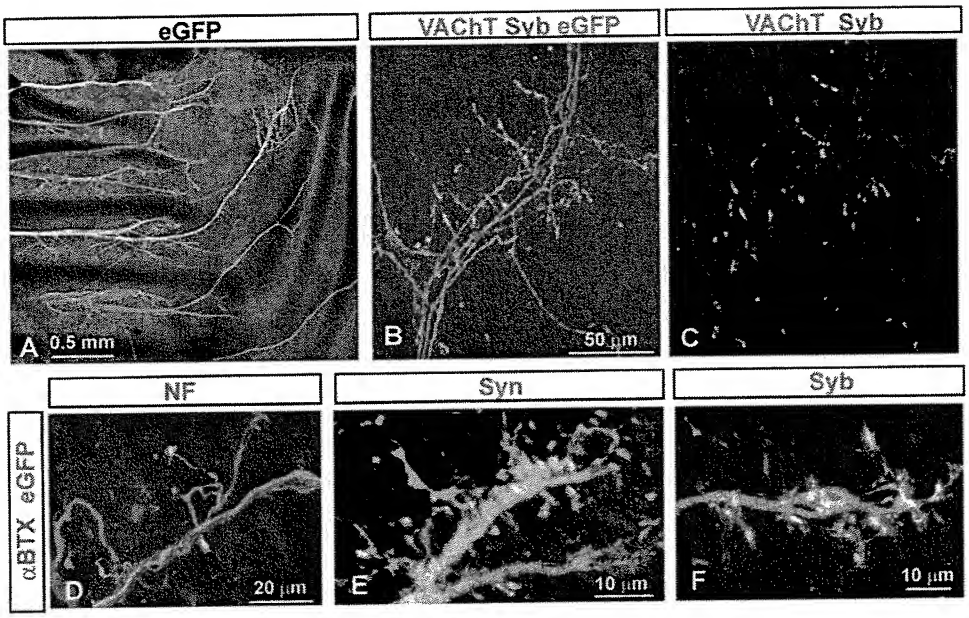

Figure 8. Synaptic Differentiation of ES Cell-Derived Motor Neurons In Vivo

(A) Whole-mount preparation of stage 35 chick embryonic rib cage. ES cell-derived eGFP$^+$ motor axons contact intercostal muscles.

(B and C) Coexpression of synaptobrevin (Syb) and vesicular ACh transporter (VAChT) in the terminals of eGFP$^+$ motor axons at sites of nerve contact with muscle. The anti-Syb and VAChT antibodies recognize mouse but not chick proteins.

(D) Neurofilament (NF) and eGFP expression in motor axons that supply intercostal muscles. eGFP$^+$ axons lack NF expression. The terminals of eGFP$^+$ axons coincide with clusters of ACh receptors, defined by α-bungarotoxin (αBTX) labeling.

(E) Coincidence of synaptotagmin (Syn) expression in eGFP$^+$ motor axon terminals and αBTX labeling.

(F) Coincidence of synaptobrevin (Syb) expression in eGFP$^+$ motor axon terminals and αBTX labeling.

ity of these cells to Hh signaling. MN generation from ES cell-derived spinal progenitors, as in vivo (Chiang et al., 1996), is completely dependent on Hh signaling. Thus, the generation of a few MNs in the absence of added Hh appears to result from expression of low levels of endogenous Hh activity in EBs, possibly mediated by Ihh or Shh (Byrd et al., 2002; Dyer et al., 2001). Conversely, elevating the level of Hh signaling in EBs markedly enhances MN generation.

A second line of evidence is provided by the profile of expression of progenitor transcription factors elicited in EBs by Hh signaling. In the absence of Hh signaling, spinal progenitors in EBs exhibit a dorsal and intermediate neural progenitor identity. Activation of Hh signaling extinguishes the expression of dorsal progenitor determinants in a concentration-dependent manner that closely mimics the response of primary spinal progenitor cells (Briscoe and Ericson, 2001). Moreover, high levels of Hh signaling activity induce the expression of Nkx6.1 and Olig2, the two progenitor cell transcription factors most intimately linked with MN generation in vivo (Sander et al., 2000; Vallstedt et al., 2001; Novitch et al., 2001; Mizuguchi et al., 2001). Together, these findings indicate that neuralized ES cells respond both to rostrocaudal and dorsoventral patterning signals in a manner that closely resembles the behavior of primary neural plate cells.

Our studies have not addressed the steps involved in the initial phase of neural differentiation from ES cells. In vivo, neural induction appears to depend on the blockade BMP signaling (Munoz-Sanjuan and Brivanlou, 2002) and exposure to FGFs (Streit et al., 2000; Wilson et al., 2000, 2001). Recent studies have suggested a role for inhibition of BMP signaling in neural induction in ES cells (Gratsch and O'Shea, 2002; Tropepe et al., 2001), but additional studies are needed to determine how closely the early steps of neural specification in ES cells conform to pathways of neural induction in vivo.

Differentiation of ES Cell-Derived Motor Neurons In Vivo

Several observations indicate that ES cell-derived MNs behave in vivo in a manner that resembles their embryonic counterparts.

First, grafted eGFP$^+$ MNs are typically found in the ventrolateral spinal cord, in a position characteristic of endogenous MNs. In contrast, ES cell-derived spinal interneurons are scattered throughout the dorsoventral axis of the spinal cord. These observations suggest that ES cell-derived MNs and interneurons undergo an active process of segregation after their introduction into the host spinal cord. An alternative possibility is that MNs that fail to populate the ventral spinal cord die or extinguish eGFP expression. One argument against this latter possibility is that MNs generated in the dorsal spinal cord in response to misexpression of Nkx6 or MNR2 proteins do survive and differentiate in an ectopic dorsal position (Tanabe et al., 1998; Briscoe et al., 2000).

Second, ES cell-derived MNs project axons out of the spinal cord via the ventral root and select the major peripheral pathways taken by somatic MNs. The projection of the axons of ES cell-derived MNs into the limb is notable, since very few of these neurons express a LIM HD code appropriate for limb-projecting LMC

neurons (Tsuchida et al., 1994). A similar mismatch between the LIM HD code of MNs and peripheral axonal trajectories is found in two other experimental contexts. Overexpression of Lhx3 confers MMC molecular identity MNs at limb levels of the spinal cord, yet many of these MNs still project axons into the limb (Sharma et al., 2000). In addition, thoracic-level MNs that have been placed at limb levels of the spinal cord can still project into the limb (O'Brien and Oppenheim, 1990). Thus, the projection of the axons of ES cell-derived MNs into the limb is likely to reflect the fact that the LIM HD code can be overridden in circumstances in which MNs face an altered or restricted choice of peripheral pathways.

Third, on arrival at target muscles, the axons of ES cell-derived MNs exhibit many signs of presynaptic differentiation, notably the expression of cholinergic neurotransmitter properties. Moreover, these presynaptic specializations are found in alignment with focal clusters of ACh receptors on the postsynaptic muscle membrane, suggesting that the synaptic contacts formed between ES cell-derived MNs and skeletal muscles are functional. Together, these in vivo studies show that ES cell-derived MNs are able to negotiate successive steps in the normal developmental program through which a newly generated MN in the spinal cord innervates its skeletal muscle target.

The efficiency with which inductive signals are able to convert ES cells into MNs suggests a general strategy for generating other predefined classes of CNS neurons, through systematic variation in the identity and concentration of patterning signals to which ES cells are exposed. The ability to direct cell fate solely through the use of extracellular factors, without the need to manipulate ES cells genetically (see, for example, Kyba et al., 2002), may permit a direct extension of this strategy to human ES cells and other classes of neural progenitor cells.

Experimental Procedures

ES Cell Culture

Wild-type (MM13 or W9.5) or HB9::GFP transgenic mouse-derived (HBG3) ES cells were grown on mouse embryonic fibroblasts in ES cell medium. ES cell colonies were partially dissociated after 2 days and cultured in DFK5 medium (see Supplemental Data at http://www.cell.com/cgi/content/full/110/3/385/DC1). Medium was replaced at 2 days and supplemented with retinoic acid (100 nM to 2 μM) (Sigma), Sonic hedgehog (Shh-N; 300 nM) (Curis Inc.), hedgehog agonist Hh-Ag1.3 (1–1000 nM) (Curis Inc.), or hedgehog antibody (5E1, 30 μg/ml), and EBs were cultured for 2–5 days. For some experiments, ES cells were grown on a PA6 cell monolayer (Riken Cell Bank, Japan) (Kawasaki et al., 2000) in DFK5 medium alone, or supplemented with 2 μM RA.

HBG3 ES cell-derived EBs were dissociated (Papain, Worthington) 4 days after induction, FACS-sorted by eGFP expression, plated on Petri dishes or Terasaki wells coated with matrigel (BD), and cultured in Supplemented F12 medium (see Supplemental Data). GDNF, NT3, CNTF, and BDNF (10 ng/ml, R&D Systems) were included in selected experiments.

Immunocytochemistry

EBs were fixed, sectioned, and processed for immunohistochemistry (Novitch et al., 2001), with antibodies noted in Supplemental Data at http://www.cell.com/cgi/content/full/110/3/385/DC1. Images were obtained using a BioRad confocal microscope.

Generation of eGFP Transgenic Mouse Lines

A transgenic mouse line was established by pronucleus injection of a ~9 kb fragment comprising the 5′ upstream region of the murine *HB9* gene (Arber et al., 1999) followed by a 5′ splice substrate (Choi et al., 1991), an *eGFP* gene, and a bovine growth hormone polyadenylation signal. In one transgenic line (*mHB9-Gfp1b*), the pattern of eGFP expression corresponded to the profile of expression of endogenous HB9. ES cell lines were derived from *mHB9-Gfp1b* heterozygous blastocysts (Abbondanzo et al., 1993). One selected line (HBG3) integrated into developing mouse blastocysts and underwent germline transmission.

FACS Isolation of HBG3 ES Cell-Derived Motor Neurons

HBG3 ES cell EBs were dissociated with papain (Worthington), and eGFP-Hi cells were sorted from the cell suspension with a Beckman-Coulter Altra flow cytometer based on eGFP fluorescence. Typically 20%–30% of input cells expressed high levels of eGFP. eGFP-Hi cells constitute a >95% pure population of MNs. The yield of a typical FACS sort is 3000–5000 GFP-Hi cells per EB.

In Vivo Transplantation of HBG3 ES Cell-Derived Motor Neurons

EBs were derived from HBG3 ES cells induced with 2 μM RA and 1 μM Hh-Ag1.3. At 3–4 days after induction, EBs were triturated and implanted into stage 15–17 chick spinal cord, which was suction-lesioned to accommodate transplanted tissue. Half to one EB equivalent was implanted into a segment spanning 2–5 somites at rostral cervical, caudal cervical, thoracic, or lumbar regions. Embryos were harvested at 3 to 7 days posttransplantation, fixed, sectioned, and labeled. For assays of axonal projection, embryos were harvested at 7 days, dissected, and labeled in wholemount with rhodamine-conjugated α-bungarotoxin (2 μg/ml, Molecular Probes) or with relevant antibodies.

Acknowledgments

We thank Barbara Han, Monica Mendelsohn, and Ira Schieren for technical help and G. Corte, R. Lovell-Badge, B. Novitch, and P. Scheiffele for antibodies. Richard Axel, Joriene de Nooij, Thomas Edlund, Johan Ericson, Vasso Episkopou, Bennett Novitch, Peter Scheiffele, and Sara Wilson provided advice and comments, and K. MacArthur valuable help, in preparation of the manuscript. H.W. is a Damon Runyon Cancer Research Fund fellow, and I.L. is supported by a HFSP postdoctoral fellowship. This work was supported by Project ALS. T.M.J. is an HHMI Investigator.

Received: May 22, 2002
Revised: July 9, 2002
Published online: July 17, 2002

References

Abbondanzo, S.J., Gadi, I., and Stewart, C.L. (1993). Derivation of embryonic stem cell lines. Methods Enzymol. *225*, 803–823.

Alvarez-Buylla, A., Garcia-Verdugo, J.M., and Tramontin, A.D. (2001). A unified hypothesis on the lineage of neural stem cells. Nat. Rev. Neurosci. *2*, 287–293.

Arber, S., Han, B., Mendelsohn, M., Smith, M., Jessell, T.M., and Sockanathan, S. (1999). Requirement for the homeobox gene Hb9 in the consolidation of motor neuron identity. Neuron *23*, 659–674.

Bain, G., Kitchens, D., Yao, M., Huettner, J.E., and Gottlieb, D.I. (1995). Embryonic stem cells express neuronal properties in vitro. Dev. Biol. *168*, 342–357.

Belting, H.G., Shashikant, C.S., and Ruddle, F.H. (1998). Multiple phases of expression and regulation of mouse Hoxc8 during early embryogenesis. J. Exp. Zool. *282*, 196–222.

Bloch-Gallego, E., Huchet, M., el M'Hamdi, H., Xie, F.K., Tanaka, H., and Henderson, C.E. (1991). Survival in vitro of motoneurons identified or purified by novel antibody-based methods is selectively enhanced by muscle-derived factors. Development *111*, 221–232.

Brazelton, T.R., Rossi, F.M., Keshet, G.I., and Blau, H.M. (2000).

From marrow to brain: expression of neuronal phenotypes in adult mice. Science *290*, 1775–1779.

Briscoe, J., and Ericson, J. (2001). Specification of neuronal fates in the ventral neural tube. Curr. Opin. Neurobiol. *11*, 43–49.

Briscoe, J., Pierani, A., Jessell, T.M., and Ericson, J. (2000). A homeodomain protein code specifies progenitor cell identity and neuronal fate in the ventral neural tube. Cell *101*, 435–445.

Byrd, N., Becker, S., Maye, P., Narasimhaiah, R., St-Jacques, B., Zhang, X., McMahon, J., McMahon, A., and Grabel, L. (2002). Hedgehog is required for murine yolk sac angiogenesis. Development *129*, 361–372.

Chiang, C., Litingtung, Y., Lee, E., Young, K.E., Corden, J.L., Westphal, H., and Beachy, P.A. (1996). Cyclopia and defective axial patterning in mice lacking Sonic hedgehog gene function. Nature *383*, 407–413.

Choi, T., Huang, M., Gorman, C., and Jaenisch, R. (1991). A generic intron increases gene expression in transgenic mice. Mol. Cell. Biol. *11*, 3070–3074.

Davis, C.A., and Joyner, A.L. (1988). Expression patterns of the homeobox-containing genes En-1 and En-2 and the proto-oncogene int-1 diverge during mouse development. Genes Dev. *2*, 1736–1744.

Durston, A.J., van der Wees, J., Pijnappel, W.W., and Godsave, S.F. (1998). Retinoids and related signals in early development of the vertebrate central nervous system. Curr. Top. Dev. Biol. *40*, 111–175.

Dyer, M.A., Farrington, S.M., Mohn, D., Munday, J.R., and Baron, M.H. (2001). Indian hedgehog activates hematopoiesis and vasculogenesis and can respecify prospective neurectodermal cell fate in the mouse embryo. Development *128*, 1717–1730.

Ericson, J., Morton, S., Kawakami, A., Roelink, H., and Jessell, T.M. (1996). Two critical periods of Sonic Hedgehog signaling required for the specification of motor neuron identity. Cell *87*, 661–673.

Ericson, J., Rashbass, P., Schedl, A., Brenner-Morton, S., Kawakami, A., van Heyningen, V., Jessell, T.M., and Briscoe, J. (1997). Pax6 controls progenitor cell identity and neuronal fate in response to graded Shh signaling. Cell *90*, 169–180.

Gage, F.H. (2000). Mammalian neural stem cells. Science *287*, 1433–1438.

Gratsch, T.E., and O'Shea, K.S. (2002). Noggin and chordin have distinct activities in promoting lineage commitment of mouse embryonic stem (ES) cells. Dev. Biol. *245*, 83–94.

Hollyday, M., and Hamburger, V. (1977). An autoradiographic study of the formation of the lateral motor column in the chick embryo. Brain Res. *132*, 197–208.

Jessell, T.M. (2000). Neuronal specification in the spinal cord: inductive signals and transcriptional codes. Nat. Rev. Genet. *1*, 20–29.

Kania, A., Johnson, R.L., and Jessell, T.M. (2000). Coordinate roles for LIM homeobox genes in directing the dorsoventral trajectory of motor axons in the vertebrate limb. Cell *102*, 161–173.

Kawasaki, H., Mizuseki, K., Nishikawa, S., Kaneko, S., Kuwana, Y., Nakanishi, S., Nishikawa, S.I., and Sasai, Y. (2000). Induction of midbrain dopaminergic neurons from ES cells by stromal cell-derived inducing activity. Neuron *28*, 31–40.

Kyba, M., Perlingeiro, R.C., and Daley, G.Q. (2002). HoxB4 confers definitive lymphoid-myeloid engraftment potential on embryonic stem cell and yolk sac hematopoietic progenitors. Cell *109*, 29–37.

Lee, K.J., and Jessell, T.M. (1999). The specification of dorsal cell fates in the vertebrate central nervous system. Annu. Rev. Neurosci. *22*, 261–294.

Lee, S.K., and Pfaff, S.L. (2001). Transcriptional networks regulating neuronal identity in the developing spinal cord. Nat. Neurosci. *4* (*Suppl.*), 1183–1191.

Lee, S.H., Lumelsky, N., Studer, L., Auerbach, J.M., and McKay, R.D. (2000). Efficient generation of midbrain and hindbrain neurons from mouse embryonic stem cells. Nat. Biotechnol. *18*, 675–679.

Liu, J.P., Laufer, E., and Jessell, T.M. (2001). Assigning the positional identity of spinal motor neurons. Rostrocaudal patterning of Hox-c expression by FGFs, Gdf11, and retinoids. Neuron *32*, 997–1012.

Lu, Q.R., Sun, T., Zhu, Z., Ma, N., Garcia, M., Stiles, C.D., and Rowitch, D.H. (2002). Common developmental requirement for Olig function indicates a motor neuron/oligodendrocyte connection. Cell *109*, 75–86.

Mallamaci, A., Di Blas, E., Briata, P., Boncinelli, E., and Corte, G. (1996). OTX2 homeoprotein in the developing central nervous system and migratory cells of the olfactory area. Mech. Dev. *58*, 165–178.

Mezey, E., Chandross, K.J., Harta, G., Maki, R.A., and McKercher, S.R. (2000). Turning blood into brain: cells bearing neuronal antigens generated in vivo from bone marrow. Science *290*, 1779–1782.

Mizuguchi, R., Sugimori, M., Takebayashi, H., Kosako, H., Nagao, M., Yoshida, S., Nabeshima, Y., Shimamura, K., and Nakafuku, M. (2001). Combinatorial roles of olig2 and neurogenin2 in the coordinated induction of pan-neuronal and subtype-specific properties of motoneurons. Neuron *31*, 757–771.

Muhr, J., Graziano, E., Wilson, S., Jessell, T.M., and Edlund, T. (1999). Convergent inductive signals specify midbrain, hindbrain, and spinal cord identity in gastrula stage chick embryos. Neuron *23*, 689–702.

Munoz-Sanjuan, I., and Brivanlou, A.H. (2002). Neural induction, the default model and embryonic stem cells. Nat. Rev. Neurosci. *3*, 271–280.

Novitch, B.G., Chen, A.I., and Jessell, T.M. (2001). Coordinate regulation of motor neuron subtype identity and pan-neuronal properties by the bHLH repressor Olig2. Neuron *31*, 773–789.

O'Brien, M.K., and Oppenheim, R.W. (1990). Development and survival of thoracic motoneurons and hindlimb musculature following transplantation of the thoracic neural tube to the lumbar region in the chick embryo: anatomical aspects. J. Neurobiol. *21*, 313–340.

Pattyn, A., Hirsch, M., Goridis, C., and Brunet, J.F. (2000). Control of hindbrain motor neuron differentiation by the homeobox gene Phox2b. Development *127*, 1349–1358.

Pevny, L., Lovell-Badge, R., and Smith, A. (1998). Generation of purified neural precursors from embryonic stem cells by lineage selection. Curr. Biol. *8*, 971–974.

Pfaff, S.L., Mendelsohn, M., Stewart, C.L., Edlund, T., and Jessell, T.M. (1996). Requirement for LIM homeobox gene Isl1 in motor neuron generation reveals a motor neuron-dependent step in interneuron differentiation. Cell *84*, 309–320.

Rathjen, J., Haines, B.P., Hudson, K.M., Nesci, A., Dunn, S., and Rathjen, P.D. (2002). Directed differentiation of pluripotent cells to neural lineages: homogenous formation and differentiation of a neurectoderm population. Development *129*, 2649–2661.

Renoncourt, Y., Carroll, P., Filippi, P., Arce, V., and Alonso, S. (1998). Neurons derived in vitro from ES cells express homeoproteins characteristic of motoneurons and interneurons. Mech. Dev. *79*, 185–197.

Reubinoff, B.E., Itsykson, P., Turetsky, T., Pera, M.F., Reinhartz, E., Itzik, A., and Ben-Hur, T. (2001). Neural progenitors from human embryonic stem cells. Nat. Biotechnol. *19*, 1134–1140.

Roelink, H., Porter, J.A., Chiang, C., Tanabe, Y., Chang, D.T., Beachy, P.A., and Jessell, T.M. (1995). Floor plate and motor neuron induction by different concentrations of the amino-terminal cleavage product of sonic hedgehog autoproteolysis. Cell *81*, 445–455.

Sander, M., Paydar, S., Ericson, J., Briscoe, J., Berber, E., German, M., Jessell, T.M., and Rubenstein, J.L. (2000). Ventral neural patterning by Nkx homeobox genes: Nkx6.1 controls somatic motor neuron and ventral interneuron fates. Genes Dev. *14*, 2134–2139.

Sharma, K., Sheng, H.Z., Lettieri, K., Li, H., Karavanuv, A., Potter, S., Westphal, H., and Pfaff, S.L. (1998). LIM homeodomain factors Lhx3 and Lhx4 assign subtype identities for motor neurons. Cell *95*, 817–828.

Sharma, K., Leonard, A.E., Lettieri, K., and Pfaff, S.L. (2000). Genetic and epigenetic mechanisms contribute to motor neuron pathfinding. Nature *406*, 515–519.

Streit, A., Berliner, A.J., Papanayotou, C., Sirulnik, A., and Stern, C.D. (2000). Initiation of neural induction by FGF signalling before gastrulation. Nature *406*, 74–78.

Tanabe, Y., William, C., and Jessell, T.M. (1998). Specification of

motor neuron identity by the MNR2 homeodomain protein. Cell *95*, 67–80.

Terada, N., Hamazaki, T., Oka, M., Hoki, M., Mastalerz, D.M., Nakano, Y., Meyer, E.M., Morel, L., Petersen, B.E., and Scott, E.W. (2002). Bone marrow cells adopt the phenotype of other cells by spontaneous cell fusion. Nature *416*, 542–545.

Thaler, J., Harrison, K., Sharma, K., Lettieri, K., Kehrl, J., and Pfaff, S.L. (1999). Active suppression of interneuron programs within developing motor neurons revealed by analysis of homeocomain factor HB9. Neuron *23*, 675–687.

Tropepe, V., Hitoshi, S., Sirard, C., Mak, T.W., Rossant, J., and van der Kooy, D. (2001). Direct neural fate specification from embryonic stem cells: a primitive mammalian neural stem cell stage acquired through a default mechanism. Neuron *30*, 65–78.

Tsuchida, T., Ensini, M., Morton, S.B., Baldassare, M., Edlund, T., Jessell, T.M., and Pfaff, S.L. (1994). Topographic organization of embryonic motor neurons defined by expression of LIM homeobox genes. Cell *79*, 957–970.

Uchida, N., Buck, D.W., He, D., Reitsma, M.J., Masek, M., Phan, T.V., Tsukamoto, A.S., Gage, F.H., and Weissman, I.L. (2000). Direct isolation of human central nervous system stem cells. Proc. Natl. Acad. Sci. USA *97*, 14720–14725.

Vallstedt, A., Muhr, J., Pattyn, A., Pierani, A., Mendelsohn, M., Sander, M., Jessell, T.M., and Ericson, J. (2001). Different levels of repressor activity assign redundant and specific roles to Nkx6 genes in motor neuron and interneuron specification. Neuron *31*, 743–755.

Wilson, S.I., and Edlund, T. (2001). Neural induction: toward a unifying mechanism. Nat. Neurosci. *4* (*Suppl*), 1161–1168.

Wilson, S.I., Graziano, E., Harland, R., Jessell, T.M., and Edlund, T. (2000). An early requirement for FGF signalling in the acquisition of neural cell fate in the chick embryo. Curr. Biol. *10*, 421–429.

Wilson, S.I., Rydstrom, A., Trimbom, T., Willert, K., Nusse, R., Jessell, T.M., and Edlund, T. (2001). The status of Wnt signalling regulates neural and epidermal fates in the chick embryo. Nature *411*, 325–330.

Wood, H.B., and Episkopou, V. (1999). Comparative expression of the mouse Sox1, Sox2 and Sox3 genes from pre-gastrulation to early somite stages. Mech. Dev. *86*, 197–201.

Ying, Q.L., Nichols, J., Evans, E.P., and Smith, A.G. (2002). Changing potency by spontaneous fusion. Nature *416*, 545–548.

Zhang, S.C., Wernig, M., Duncan, I.D., Brustle, O., and Thomson, J.A. (2001). In vitro differentiation of transplantable neural precursors from human embryonic stem cells. Nat. Biotechnol. *19*, 1129–1133.

Zhou, Q., and Anderson, D.J. (2002). The bHLH transcription factors OLIG2 and OLIG1 couple neuronal and glial subtype specification. Cell *109*, 61–73.